Molecular Therapy
Methods & Clinical Development
Original Article

Evaluation of anti-vector immune responses to adenovirus-mediated lung gene therapy and modulation by αCD20

Robert D.E. Clark,[1] Felix Rabito,[1] Ferris T. Munyonho,[1] T. Parks Remcho,[1] and Jay K. Kolls[1]

[1]Departments of Pediatrics & Medicine, Center for Translational Research in Infection and Inflammation, Tulane University School of Medicine, New Orleans, LA 70112, USA

Although the last decade has seen tremendous progress in drugs that treat cystic fibrosis (CF) due to mutations that lead to protein misfolding, there are approximately 8%–10% of subjects with mutations that result in no significant CFTR protein expression demonstrating the need for gene editing or gene replacement with inhaled mRNA or vector-based approaches. A limitation for vector-based approaches is the formation of neutralizing humoral responses. Given that αCD20 has been used to manage post-transplant lymphoproliferative disease in CF subjects with lung transplants, we studied the ability of αCD20 to module both T and B cell responses in the lung to one of the most immunogenic vectors, E1-deleted adenovirus serotype 5. We found that αCD20 significantly blocked luminal antibody responses and efficiently permitted re-dosing. αCD20 had more limited impact on the T cell compartment, but reduced tissue resident memory T cell responses in bronchoalveolar lavage fluid. Taken together, these pre-clinical studies suggest that αCD20 could be re-purposed for lung gene therapy protocols to permit re-dosing.

INTRODUCTION

Cystic fibrosis (CF) is a devastating genetic disease caused by autosomal recessive mutations in the cystic fibrosis transmembrane receptor (CFTR) chloride channel, loss of which results in dysregulation of epithelial water homeostasis.[1] Although CFTR is widely expressed, people with CF (pwCF) experience the greatest morbidity and mortality from lung disease.[2] Nonfunctional CFTR leads to thickened airway secretions, impairing mucociliary clearance and causing consequent acquisition of recurrent, severe sinopulmonary infections.

Approximately 2,000 different CFTR mutations have been described and are classified into 6 categories based on biochemical characteristics.[3] Many of these mutations that permit some degree of protein expression are now able to be targeted by CFTR potentiator and corrector drugs, which function by promoting proper folding and intracellular transport of the CFTR protein.[4–6] Despite the marked success of drugs that correct misfolded CFTR,[5] there are at least 8%–10% of CF subjects with currently undruggable mutations. Furthermore, current therapies do not fully restore lung function even for those pwCF with druggable mutations.[7] Thus, there is much effort to explore other options such that no patient with CF is "left-behind" in the era of protein modulator therapy, including mRNA and vector-based approaches for gene replacement or gene editing. Many of the approaches currently envisioned will require administration of non-host proteins to the lung and there are concerns that targeting efficiency must be high, given that re-dosing may not be feasible.

Inhaled vector-based gene therapy is one approach to target undruggable mutations. Gene therapy has several advantages over currently available drugs; most significantly, gene therapy can target any class of mutation. Several gene therapy trials for CF have been carried out; however, none have thus far been successful.[8] Since the early trials of viral-based gene therapy in the 1990s, in the field it was realized that viral vectors could elicit both B and T cell immune responses in the lung,[9] which may eliminate and prevent re-administration of the viral gene therapies and cause insufficient and transient correction.[10] In addition, in these early studies, our knowledge of the pulmonary immune system was fairly rudimentary. During these early trials there were largely only two subsets of T cells under consideration, Th1 and Th2 cells, whereas now there are additional subsets including Th17 cells, T follicular helper (Tfh) cells, Th9 cells, and regulatory T cells.[11] Moreover, in addition to B cells being primed in draining lymph nodes, there are novel data that both the resident memory B cells (B_{RM})[12] and plasma cells can reside locally in the lung.[13] In addition to antigen trafficking to hilar lymph nodes, immune responses can occur in tertiary lymphoid structures such as inducible bronchial-associated lymphoid tissue, or iBALT,[14] which is present in the CF lung.[15] However, despite the knowledge that immune responses represent a primary barrier to effective gene therapies, mucosal immune responses to gene therapy vectors have thus far only been poorly characterized. In particular, the ability of gene therapy vectors to elicit B_{RM} and T-resident memory (T_{RM}) cells

Received 16 August 2023; accepted 21 June 2024;
https://doi.org/10.1016/j.omtm.2024.101286.

Correspondence: Jay K. Kolls, PhD, Departments of Pediatrics & Medicine, Center for Translational Research in Infection and Inflammation, Tulane University School of Medicine, New Orleans, LA 70112, USA.
E-mail: jkolls1@tulane.edu

Published by Elsevier Inc. on behalf of The American Society of Gene and Cell Therapy.
This is an open access article under the CC BY-NC-ND license (http://creativecommons.org/licenses/by-nc-nd/4.0/).

has not been studied. B_{RM} and T_{RM} are lung-resident cells that reside in lung parenchyma and respond rapidly to antigen re-exposure, preventing dissemination of pathogens but also potentially blocking re-delivery of gene therapy vectors.

Repeated administration of gene therapy vectors has the potential to overcome low correction efficiencies and transient expression. Recent work with systemically administrated vectors has examined the potential of agents targeting humoral immunity, and various strategies to minimize vector neutralization by transient reduction of all[16,17] or vector-specific[18,19] immunoglobulins (Igs) have met with at least partial success. T cell-mediated rejection is also a known concern for viral gene therapy vectors,[20] and various strategies are being assessed to prevent or reduce anti-vector T cell responses.[21] Recently, there have been advances in a number of targeted therapies for autoimmune diseases that are in part due to the generation of autoantibodies, including αCD20 as well as enzymes that can cleave human Igs.[16,17] Given that αCD20 is currently used in CF subjects for pre-transplant high-HLA sensitization[22] and to manage post-transplant lymphoproliferative disease and appears to be well tolerated,[23,24] we investigated αCD20's effects on adaptive immune response in the lung to viral-based gene therapy. Furthermore, in terms of cell-mediated immunity, the lung is a unique mucosal niche where, in addition to dendritic cells, B cells play key roles as antigen-presenting cells. Our prior work showed that depletion of B cells with αCD20 abrogates priming of lung memory CD4+ T cell responses to the fungus *Pneumocystis murina*.[25]

Here, we describe the mucosal immune response to inhaled gene therapy vector delivery in the presence and absence of B cell depletion by αCD20 treatment. We selected E1-deleted adenovirus serotype 5 (HAdV) vectors as a proof of concept due to their well-known ability to elicit potent immune responses, reasoning that if our strategy showed efficacy in this context, it might also show efficacy with more clinically relevant and less immunogenic vectors such as adeno-associated viruses (AAVs).

We found that inhaled HAdV vector delivery elicited lung resident B_{RM} and T_{RM}. The administration of αCD20 prior to primary vector delivery reduced formation of anti-HAdV B_{RM} and Igs in serum and bronchoalveolar lavage fluid (BALF). We also found some effects of αCD20 treatment on lung T_{RM} formation, with a shift in proportions of CD8+ T_{RM} subsets and reduced numbers of airway T cells in BALF with the higher dose αCD20 arm. Both high and low doses of αCD20 prior to primary vector delivery rescued secondary gene transfer at 4 weeks to a level similar to that of vector-naive mice. However, only high-dose αCD20 was able to fully restore secondary gene transfer when re-dosing at 6 weeks after recovery of circulating B cells. In addition, second-round vector administration was permissive in $AID^{-/-}\mu S^{-/-}$ mice that are deficient in all secreted Igs, but not in $FcRn^{-/-}$ (the receptor that transports IgG to the alveolar space) or $IgA^{-/-}$ mice. Together, these data indicate that luminal Igs are a key mechanism of impaired secondary adenoviral-mediated gene transfer and that modulation of host immune responses prior to gene therapy vector delivery may be a promising strategy to permit repeated dosing and improved treatment efficacy.

RESULTS

αCD20 treatment impairs B cell-mediated immune responses to adenoviral vector delivery

To assess anti-vector memory immune responses, we dosed mice with αCD20 or IgG2a isotype controls, and 2 days later delivered a luciferase-expressing HAdV vector to the lungs of mice by oropharyngeal aspiration and analyzed lung immune responses after 1 month (Figure 1A). To optimize the dosage of αCD20 antibody needed to maintain B cell depletion for the duration of the experiment, mice received either 100 or 200 μg of αCD20 antibody via intraperitoneal injection. B cell depletion was monitored by flow cytometric analysis of peripheral blood at day 0, and 7, 14, or 28 days post HAdV vector delivery (Figures S1A and S1B). We found that 200 μg of αCD20 antibody maintained B cell depletion over the study period (Figure S1B). In contrast, mice treated with 100 μg of αCD20 antibody began to recover peripheral blood B cells near the end of the study period (Figure S1B). There was no perturbation in the number of peripheral blood CD4+ or CD8+ T cells among any of the groups relative to age-matched specific pathogen-free (SPF) naive mice (Figure S1B).

To examine the impact of B cell depletion on humoral immune responses, we evaluated HAdV-specific Igs in serum and BALF 28 days post vector delivery. We first determined that single-point dilution optical density was well-correlated with half-maximal effective concentration (EC_{50}) titer determined by serial dilution (Figure S1C), and therefore used single-point dilutions to evaluate subsequent samples, a method which has been rigorously validated in the context of other viruses.[26] αCD20 treatment was unable to fully prevent the formation of HAdV-specific IgG in serum at day 28 post vector administration. In contrast to serum, anti-HAdV IgA and IgG in BALF were substantially reduced to undetectable levels (Figure 1B). We were unable to detect anti-HAdV IgA in serum of any groups at a dilution of 1:32, indicative of the more minor role IgA plays in systemic versus mucosal immunity. Based on this, we also used flow cytometry to evaluate the generation of tissue-resident B cells (B_{RM} cells), after HAdV vector delivery, in the lung and BALF, using intravascular (i.v.) staining[27] to discriminate between cells present in the blood and lung parenchyma. Using this technique, we found that the residency marker CD69 was restricted to lung $i.v.CD45^{-}$ B cells (Figure S1D). αCD20 treatment prevented the development of class-switched B_{RM} cells in lung defined as $i.v.CD45^{-}CD19^{+}IgD^{-}IgM^{-}CD69^{+}$ cells[12,13] after HAdV treatment to levels at or below those observed in age-matched naive SPF mice (Figure 1C). In the BALF, we observed a similar reduction in the number of B cells (Figure 1C). Antigen-specific responses were also evaluated by B cell ELISPOT. We observed a significant amount of background in this assay, which we believe is due to polyclonal stimulation of mouse lung cells activating naive mouse B cells to produce antibodies reacting with broadly recognizable epitopes on HAdV-coated plates. At 4 weeks after HAdV delivery, isotype-treated mice had substantially increased numbers of HAdV-specific IgG- and IgA-secreting B cells

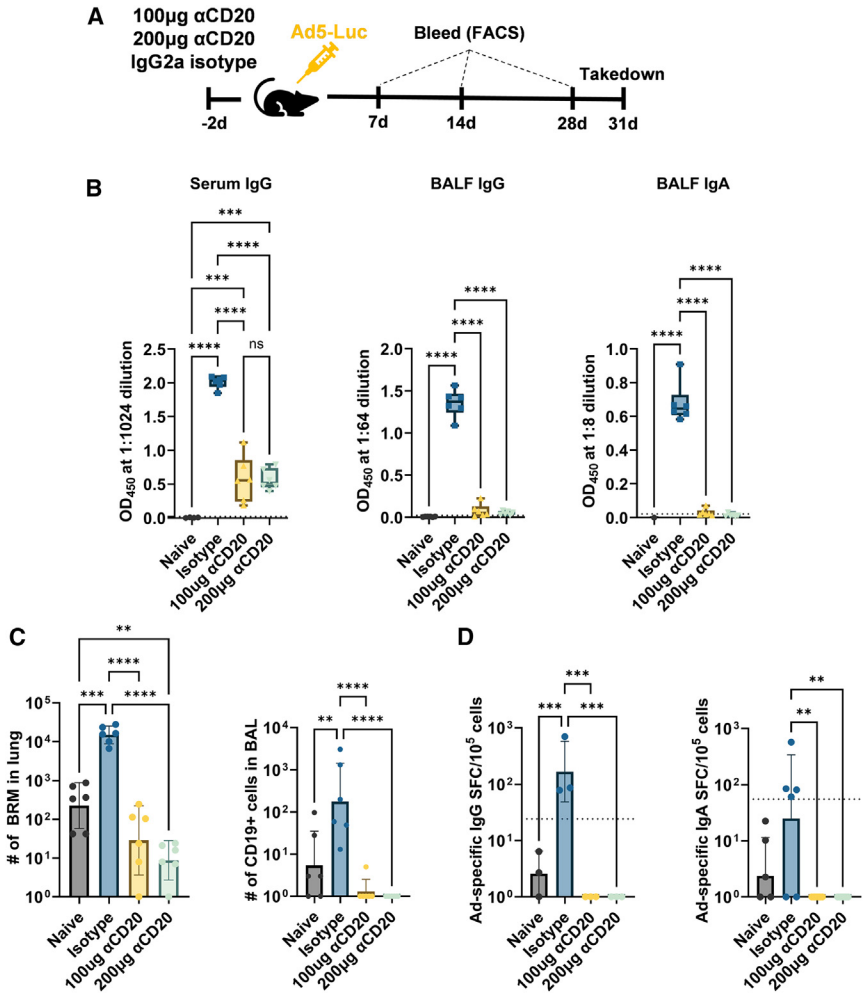

Figure 1. B cell-mediated immune response to adenoviral vector delivery

(A) Schematic of experimental timeline. Mice were treated with 100 or 200 µg of αCD20 antibody or mouse IgG2a isotype control 2 days prior to vector delivery by oropharyngeal aspiration, followed by euthanasia 4 weeks later. Naive mice received no antibody or HAdV treatment. (B) ELISA analysis of anti-adenovirus IgG in serum (left) and IgA (middle), and IgG (right) in BALF. (C) Enumeration of total B-resident memory lymphocytes (i.v.CD45$^-$ CD19$^+$IgD$^-$IgM$^+$CD69$^+$) in lung (left) and CD19$^+$ cells in BAL fluid (right). (D) Enumeration of adenovirus-specific IgG (left) and IgA (right) secreting cells. Dotted lines indicate the mean + 3 SD of naive control mice. $^*p < 0.05$, $^{**}p < 0.01$, $^{***}p < 0.001$, $^{****}p < 0.0001$ by one-way ANOVA. Data shown are mean ± SD; $n \geq 3$ mice per group; representative of 2 independent experiments.

in the lung as compared with naive controls (Figure 1D). However, pre-treatment with either dose of αCD20 reduced the number of HAdV-specific IgG- and IgA-secreting B cells to the level of naive controls (Figure 1D).

Adenoviral vector delivery elicits lung T_{RM} cells

To characterize the T cell population in the mouse lung 1 month after HAdV dosing, we isolated i.v.CD45$^-$CD3$^+$ T cells from mice 4 weeks after HAdV dosing and performed single-cell TCR sequencing and gene expression analysis. TCR sequences from HAdV-dosed mouse lung were highly oligoclonal compared with sequences from naive spleen (Figure 2A). Analysis of the top 5 most common clonotypes revealed that the most expanded clones were primarily CD8+ T cells (Figure 2B). Gene expression clustering of lung and naive spleen CD8+ T cells revealed four main clusters, with most lung cells separating clearly from naive spleen cells and falling into cluster 2 (Figure 2C). Cluster 2 exhibited the highest expression levels of CD8+ T_{RM} markers *Cd69*,[28–30] *Itgae* (CD103),[28–30] and *Itga1* (CD49a) (Figure S2A), and the lowest expression levels of *S1pr1* and *Klf2*, which are downregulated in T_{RM},[31] indicating that cluster 2 contains T_{RM} (Figure S2B). A similar analysis was carried out for CD4+ T cells, with lung cells again clustering differently from spleen cells, this time falling in clusters 3 and 5 (Figure S2C). CD4+ T_{RM} markers are less well defined compared with CD8+ T_{RM},[31–33] and analysis of markers *CD69*, *Itga1* (CD49a), *Zfp683* (Hobit), and *Eomes* revealed relatively high levels among all clusters (Figure S2D). However, expression levels of *S1pr1* and *Klf2* were lowest in clusters 3 and 5, indicating the presence of T_{RM} (Figure S2E). We also sought to understand differences among CD4+ lung T_{RM} clusters 3 and 5 by examining the expression of Th subset lineage markers (Figure S2F). Cluster 3 was enriched in *Ifnγ*-expressing Th1 cells and cluster 5 in *Il17a*-expressing Th17 cells, whereas relatively few cells in these clusters expressed Th2 or Tfh markers *Il4* and *Cxcr5*, respectively (Figure S2F). However, in evaluating TCR sequences, only the Th1-enriched cluster 3 contained clonally expanded cells (Figure S2G).

Impact of αCD20 treatment on T cell-mediated immune responses to adenoviral vector delivery

As B cells can also function as APCs in the lung for T cell responses, we further evaluated the memory T cell response to HAdV delivery. Similar to the B_{RM} cells, CD69 expression was restricted to lung parenchymal i.v.CD45$^-$ T cells; however, expression of the T_{RM} marker CD103 was observed on some lung and intravascular CD45-labeled cells (Figure S3A). Relative to age-matched naive SPF mice, mice dosed with HAdV exhibited increased numbers of parenchymal i.v.CD45$^-$ T cells (Figure 3A). However, no major differences were observed in the numbers of CD4+ or CD8+ T_{RM} cells within varying subsets defined by CD69 and CD103 expression among HAdV-dosed mice with or without αCD20 treatment. Despite the lack of observed alteration in absolute numbers of T_{RM} with

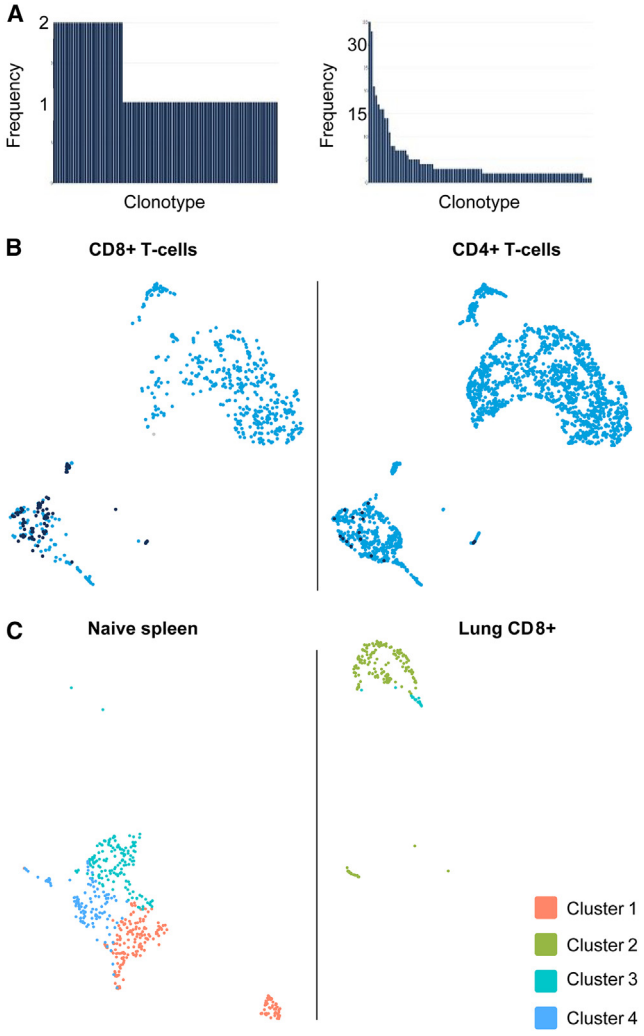

Figure 2. Single-cell sequencing identifies lung-resident T_{RM}

(A) Clonotype frequency of T cells in naive spleen (left) and lung 1 month after HAdV delivery (right). (B) Distribution of top 5 most observed clonotypes among CD4+ and CD8+ T cells. Dark puncta indicate cells that contain one of the top 5 most expanded TCR sequences. (C) UMAP gene expression clustering of CD8 T cells in naive spleen (left) and lung 1 month after HAdV delivery (right).

αCD20 treatment, within the CD8+ compartment there was a reduction in the frequency of $CD69^{+}CD103^{+}$ T_{RM} cells (Figure 3B). Moreover, there was a distinct reduction in the number of T cells of all subsets in BALF with αCD20 treatment, with the number of BALF T cells in 200 μg αCD20-treated, HAdV-dosed mice only slightly greater than the number found in naive SPF mice (Figure S3B). Antigen-specific T cell responses were assessed by ELISPOT after stimulation with the dominant H2-K^{b} epitopes for adenovirus[34] and luciferase.[35] No difference was observed in the IFN-γ response to peptide stimulation for either antigen (Figure 3C) between control and αCD20-treated mice. We assayed the supernatant of the stimulated wells for cytokine production using a LegendPlex multiplex assay to assay type 1, type 2, and type 17 responses. Interestingly, IL-22 production was significantly lower in cells from mice treated with 200 μg of αCD20 and there was a trend toward lower levels of other type 17 cytokines (Figure 3D). In contrast, levels of type 1 and type 2 cytokines were broadly similar between groups (Figure S3C).

αCD20 treatment permits vector re-dosing in the lung, similar to Ig-deficient mice

After characterizing the first-round immune response, we sought to determine whether αCD20 treatment could permit re-dosing of HAdV. Similar to prior experiments, mice were dosed with varying doses of αCD20 or isotype control 2 days prior to oropharyngeal delivery of a GFP-expressing HAdV. Four weeks later, mice were challenged with a second-round β-galactosidase-expressing HAdV and euthanized after 3 days assay of secondary gene transfer (Figure 4A). Isotype-treated mice had approximately 50% reduced transgene activity as compared with vector-naive mice. However, pre-treatment with both 100 and 200 μg of αCD20 were able to rescue secondary gene transfer (Figure 4B) to ∼90% of the level of vector-naive mice. Despite near-complete rescue of transgene activity, qPCR analysis indicated only partial rescue of vector genome copy number after re-dosing, even with αCD20 treatment (Figure S4A). Anti-β-gal IHC revealed the greatest levels of staining in the conducting airways, confirming transduction of cells relevant for the treatment of CF and primary ciliary dyskinesia (Figure 4C).

We also sought to understand whether transient αCD20 would provide a benefit to re-dosing after reconstitution of peripheral blood B cells. Cohorts of mice were dosed with either low (100 μg) or high (200 μg) doses of αCD20 or isotype control, and one group of low-dose αCD20 mice did not receive a second dose of vector, to permit study of the impact of the second dose of HAdV on immune responses. To accomplish this, we monitored mouse peripheral blood by flow cytometry for B cell reconstitution starting 1 month after primary vector delivery (Figure 4D). B cells in the low-dose αCD20-treated mice recovered approximately 4 weeks after αCD20 dosing initiation, and the high-dose cohort had near-complete reconstitution of circulating B cells by 6 weeks. Of note, in this experiment, we observed greater variability in IgG responses and a more rapid reconstitution of the B cell compartment was observed in the low-dose αCD20 cohort than observed previously (Figure S1B). The re-emergence of circulating B cells was associated with an increase in serum anti-HAdV IgG in the low-dose cohort but not in the high-dose αCD20-treated mice (Figure S4C). In all cohorts receiving primary vector administration, serum anti-HAdV IgG was detectable above background starting at 2 weeks after HAdV delivery, and these antibodies increased rapidly until 4 weeks, and then more gradually thereafter (Figure S4C). Prior treatment with αCD20 resulted in a delayed rise in serum anti-HAdV IgG in both low- and high-dose cohorts (Figure S4C). Area under the curve analysis revealed that mice receiving a high dose of αCD20 had substantially reduced anti-HAdV antibody responses over the study period (Figures 1B, S4D, and S4E). To assess efficiency of gene transfer in B cell-reconstituted mice, animals were re-dosed with Ad-LacZ 2 weeks after full

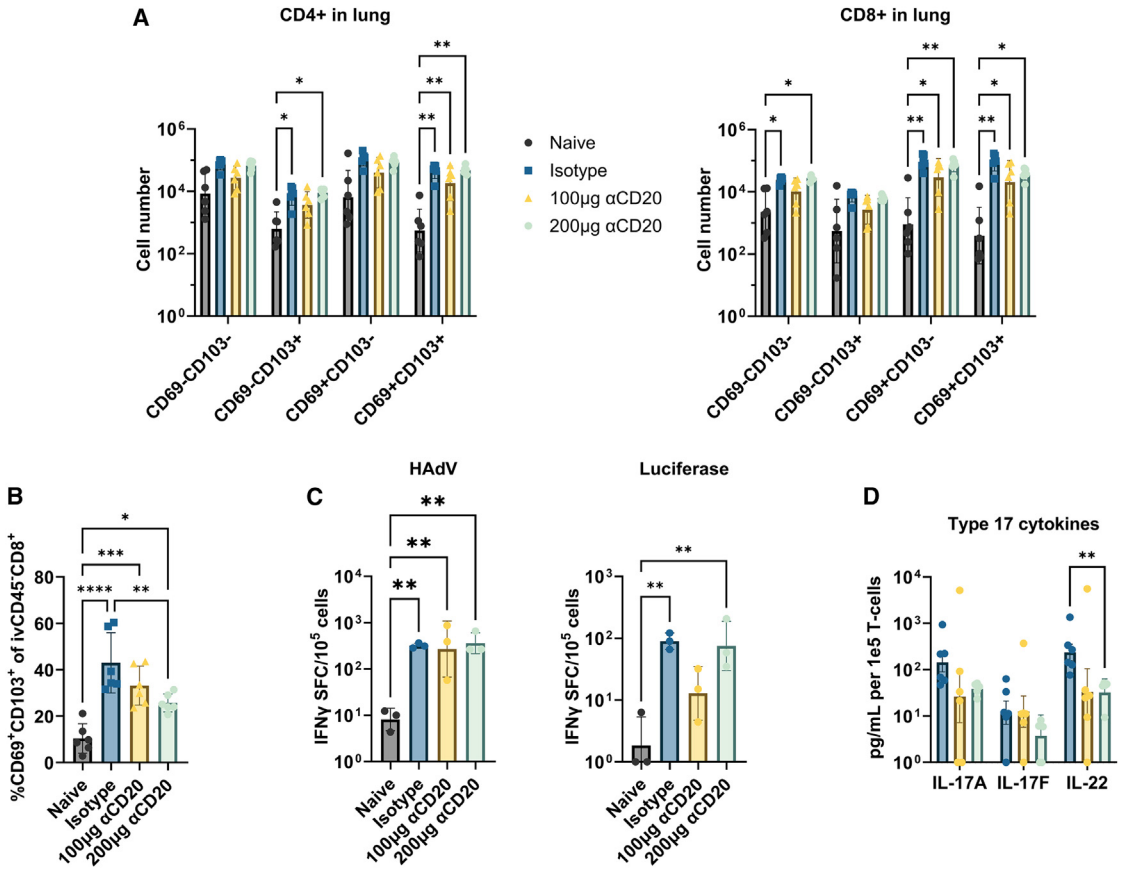

Figure 3. T cell responses to adenoviral vector delivery

Mice were treated as in Figure 1. (A) Enumeration of total lung extravascular CD4+ (i.v.CD45$^-$CD4$^+$) and CD8+ (i.v.CD45$^-$CD8$^+$) T_{RM} subsets. *$p < 0.05$, **$p < 0.01$ by two-way ANOVA. (B) Percentage of CD69$^+$CD103$^+$ cells among i.v.CD45$^-$CD8$^+$ cells. *$p < 0.05$, **$p < 0.01$, ***$p < 0.001$, ****$p < 0.0001$ by one-way ANOVA. (C) Enumeration of IFN-γ-secreting cells responsive to HAdV (left) and luciferase (right) peptide stimulation. *$p < 0.05$, **$p < 0.01$, ***$p < 0.001$, ****$p < 0.0001$ by one-way ANOVA. (D) Cytokine secretion in response to peptide stimulation. **$p < 0.01$ by two-way ANOVA. Data shown are mean ± SD; $n \geq 3$ mice per group; representative of 2 independent experiments.

reconstitution. Three days after secondary gene transfer, high-dose but not low-dose αCD20 significantly reduced BAL anti-HAdV IgG relative to isotype-treated mice, similarly to serum IgG (Figure S4E). In contrast, BAL IgA was significantly reduced in all αCD20 groups, although anti-HAdV BAL IgA (above background) was detectable in 5/10 mice dosed with 100 µg αCD20 (Figure S4E). We did not observe any difference in Ig responses between low-dose αCD20 groups which did or did not receive the second vector. Assessment of β-galactosidase transgene activity in lung homogenate revealed that isotype-treated mice had reduced transgene expression to 75% of vector-naive mice. Low- and high-dose αCD20 restored β-galactosidase activity in lung homogenate to 81% and 94% of activity in vector-naive controls, respectively (Figure 4E). However, these differences did not reach statistical significance. While these results indicated some benefit for αCD20 in re-dosing, greater variability than observed previously and higher second-round gene transfer in the isotype group limited the power of our statistical analysis to resolve differences among groups (Figure 4E).

Given the small impact of αCD20 treatment on lung parenchymal T cell-mediated immune responses to the delivered adenoviral vectors, we focused on Igs to elucidate the mechanism by which αCD20 treatment permits vector re-dosing.[36] Several genetically modified mouse lines were used, including IgA$^{-/-}$ mice, which do not make standard or secretory IgA, FcRn$^{-/-}$ mice, which lack the neonatal Fc receptor that is highly expressed in in lung distal type I and type II pneumocytes and is responsible for transport of IgG across many epithelial tissues,[37] and AID$^{-/-}$uS$^{-/-}$ mice, which lack any secreted Igs while possessing a full repertoire of low-affinity membrane-bound immature B cell receptors.[38] Of note, the COVID-19 cell atlas shows that *FCGRT* (FcRn) expression in the lung is largely restricted to the alveolar epithelium.[39] Similar to previous experiments, mice were dosed initially with a first-round empty vector and then re-dosed with a second-round luciferase-expressing HAdV (Figure 5A). Re-dosing was possible in αCD20-treated mice and AID$^{-/-}$uS$^{-/-}$ mice, with secondary gene transfer levels indistinguishable from mice receiving the second HadV only (Figure 5B).

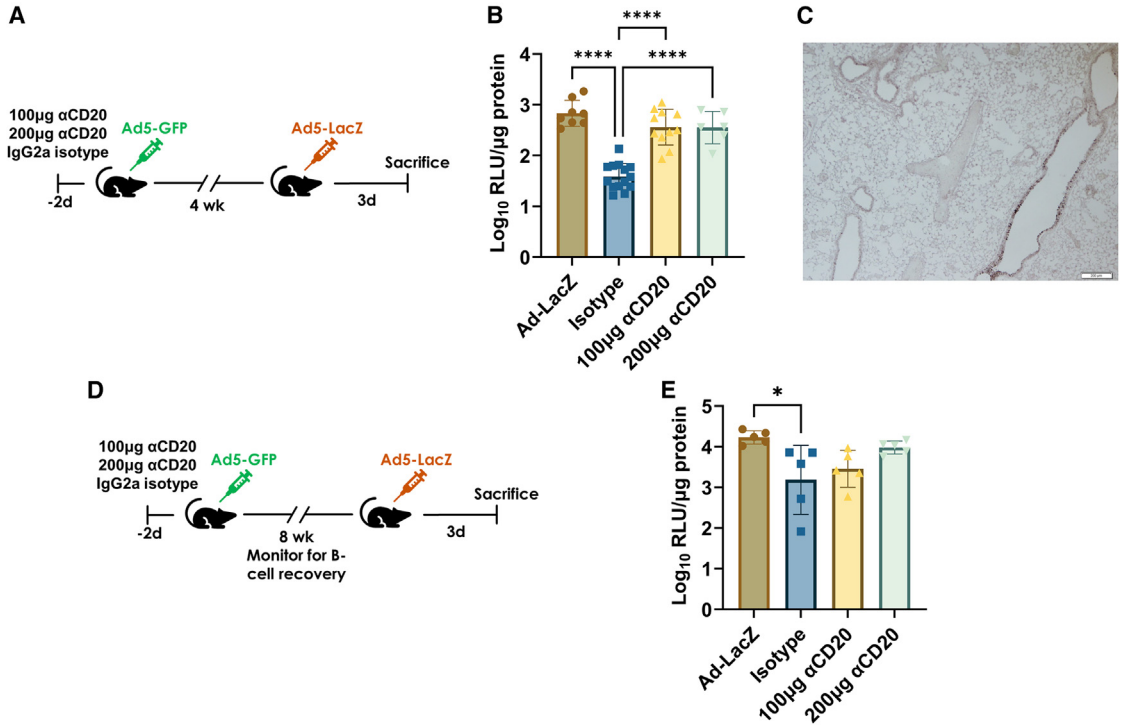

Figure 4. αCD20 treatment permits efficient vector re-administration

(A) Schematic of repeat-dose experimental design. One hundred or 200 µg of αCD20 antibody or mouse IgG2a isotype control 2 days prior to vector delivery by oropharyngeal aspiration. Four weeks later, mice were re-dosed with a second vector, also by oropharyngeal aspiration and euthanized 3 days later. Ad-LacZ control mice received only the second dose of HAdV. (B) Quantification of β-galactosidase activity in lung homogenate, assayed by Gal-Screen chemiluminescent activity assay. (C) Representative image of IHC staining for β-galactosidase. Scale bar, 200 µm. (D) Schematic of repeat-dose experimental design after B cell recovery. Groups are the same as in (A), with the inclusion of one group of mice treated with 100 µg αCD20 that did not receive the Ad-LacZ vector (Figure S4). (E) Quantification of β-galactosidase activity in lung homogenate, assayed by Gal-Screen chemiluminescent activity assay. *$p < 0.05$, ****$p < 0.0001$ by one-way ANOVA. Data shown are mean ± SD; $n \geq 4$ mice per group; data combined from 3 independent experiments.

IgA$^{-/-}$ and FcRn$^{-/-}$ mice had substantially reduced levels of secondary gene transfer that were indistinguishable from wild-type (WT) mice (Figure 5B). Analysis of anti-adenovirus Igs in serum and BALF revealed expected patterns, with a lack of IgA in IgA$^{-/-}$ mice and a lack of all secreted Igs in AID$^{-/-}$uS$^{-/-}$ mice (Figure 5C). However, FcRn$^{-/-}$ mice had BALF IgG levels equivalent to WT mice, suggesting the neonatal Fc receptor is not critical for transport of IgG into the airway lumen in this context (Figure 5C). One possible explanation for this is HAdV-driven inflammation leading to increased barrier permeability of and paracellular transport of IgG.[40,41] Of note, the single αCD20-treated mouse with higher levels of anti-HadV serum IgG and detectable BALF IgG had somewhat lower levels of secondary gene transfer despite undetectable BALF IgA (Figure 5C). Overall, αCD20-treated mice phenocopied AID$^{-/-}$uS$^{-/-}$ mice in the repeated dosing experiments, revealing a critical role for secreted Igs as a barrier to vector re-dosing.

Flow cytometric analysis of BALF 3 days after gene transfer revealed an increased number of airway CD19^{+} and B_{RM} cells relative to mice receiving the second vector only, although αCD20 treatment greatly reduced the number of airway B lymphocytes in all conditions (Figure S5A). Similar trends were observed for airway CD4+ and CD8+ T_{RM} in all conditions except for AID$^{-/-}$uS$^{-/-}$ mice, which had similar numbers of airway cells to mice receiving only the second gene transfer vector (Figure S5B). We also evaluated the number of T lymphocytes in the lung of AID$^{-/-}$uS$^{-/-}$ compared with similarly treated WT controls (Figure S5C). There was a notable increase in CD69^{-} CD4+ T cells with a concomitant decrease in CD69^{+} CD8+ T cells (Figure S5C), yielding a significantly increased CD4+/CD8+ ratio (Figure S5D). A similarly increased CD4+/CD8+ ratio was observed in the BALF of AID$^{-/-}$uS$^{-/-}$ mice (Figure S5D). However, no other treatment conditions displayed cell subset perturbations relative to WT mice.

DISCUSSION

Gene therapy has long held great promise for the ability to treat severe monogenetic diseases such as CF.[8,10] However, thus far immune responses have often precluded treatment efficacy, with the earliest effective gene therapy treatments featuring delivery to immune-privileged sites (Luxturna, Zolgensma). Immune modulation has thus emerged as an avenue to promote safe and efficacious gene therapy when delivered to immune-competent sites.[42] For example, most

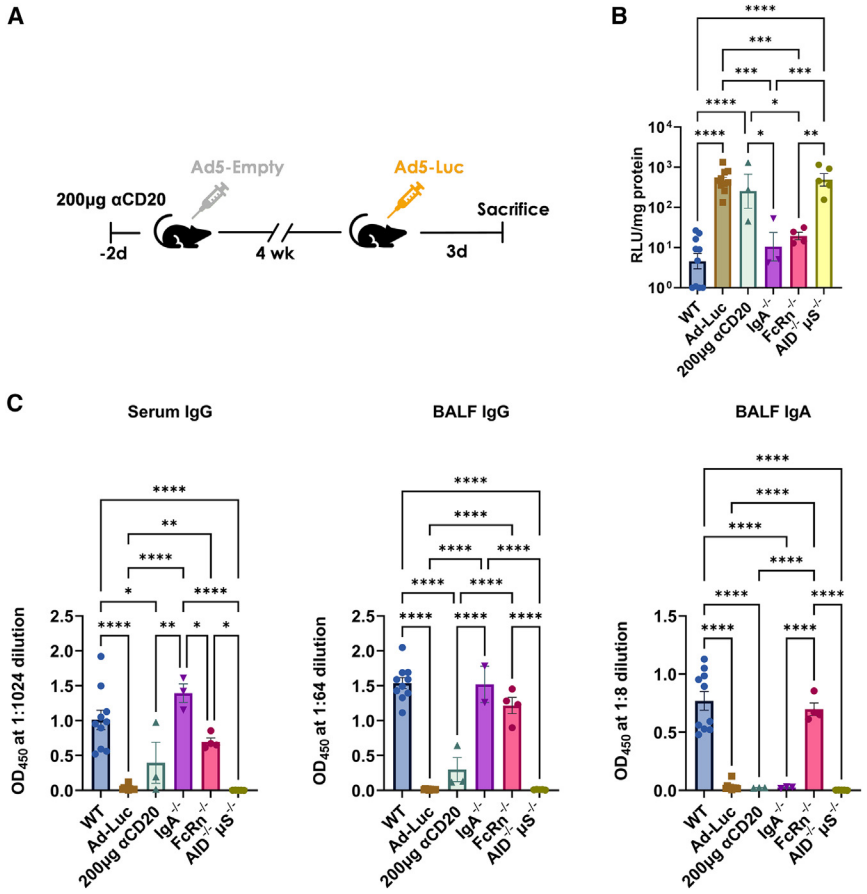

Figure 5. AID$^{-/-}$μS$^{-/-}$ mice, but not FcRn$^{-/-}$ or IgA$^{-/-}$ mice are permissive to re-dosing with adenoviral vectors

(A) Schematic of repeat-dose experimental design. Viruses were administered by oropharyngeal aspiration as in Figure 4A. All mice received two doses of HAdV other than Ad-Luc control mice, which received only the second dose. Group names indicate mouse strain genotype on the C57BL/6 background, other than parental strain (C57BL/6) WT and αCD20-treated mice. (B) Quantification of luciferase activity in lung homogenate, normalized to total protein content by One-Glo luciferase and BCA assays. *p < 0.05, **p < 0.01, ***p < 0.001, ****p < 0.0001 by one-way ANOVA. (C) OD450 of serum IgG (left), BAL IgG (middle), and BAL IgA (left). *p < 0.05, **p < 0.01, ***p < 0.001, ****p < 0.0001 by one-way ANOVA. Data shown are mean ± SD; $n \geq 3$ mice per group. Data are pooled from 3 individual experiments.

patients receiving the recently approved hemophilia A treatment Valoctocogene roxaparvovec also receive corticosteroids to manage host immune responses and transient increases in liver enzymes.[43]

Most studies of immune modulation to improve gene therapy efficacy have taken place in the context of systemic vector administration. However, lung-directed gene therapy is likely to present unique difficulties. Unlike liver and muscle, the lung is a site of frequent pathogen encounter, and extensive evolutionary mechanisms have developed to prevent infection. These mechanisms include secretion of mucosal Igs, the formation of T_{RM} and B_{RM}, and differential receptor expression on apical and basolateral airway surfaces.[44,45] Thus, mucosal immune responses in the lung are likely to present unique challenges to gene therapy vector delivery, especially for viral vectors.

Despite this concern, immune responses to inhaled gene therapy vectors remain understudied in recent years, even as techniques such as intravascular staining[27] have enhanced our understanding of immunity in the lung.[46] In this study, we selected HAdV vectors due to their potent ability to elicit immune responses, reasoning that approaches able to permit re-dosing in a highly immunogenic context may be repurposed for less immunogenic, more clinically relevant AAV vectors. However, we recognize the limitations of this approach given the unique nature of host-virus interactions and future work will seek to extend our findings to other contexts.

Our results suggest that αCD20 treatment may be of utility in prevention of mucosal immune responses in the context of inhaled gene therapy. αCD20 treatment was unable to completely prevent the formation of an anti-vector serum IgG response, similar to what is observed for other pathogens[47] and systemically administered AAV vectors.[48] However, αCD20 treatment did largely prevent the formation of luminal IgG and IgA antibodies measured in BALF and rescued second-round gene transfer. HAdV re-delivery efficiency for αCD20-treated mice also phenocopied AID$^{-/-}$μS$^{-/-}$ mice lacking secreted Igs and mature B cell receptors. Together, these data indicate a critical role for luminal Igs in preventing lung-directed re-dosing and suggest αCD20 may be better able to prevent formation of luminal versus systemic Igs upon antigen encounter. B cell depletion by αCD20 antibodies is circulation dependent, with opsonized cells removed by liver Kupffer cells.[49] B cells in bone marrow are less efficiently depleted than blood cells, perhaps due to less frequently entering circulation,[50] and exposure of bone marrow B cells to circulating HAdV antigens may elicit production of circulating anti-HAdV IgG. In contrast, lung B_{RM} are recruited from circulating cells by local antigen encounter and contribute to secretion of airway Igs,[12,13] providing a rationale for the greater observed impact of αCD20 treatment on airway Igs. In support of this mechanism of action, transient αCD20 treatment suppressed anti-HAdV airway IgA even after full B cell reconstitution.

In our experiment re-dosing HAdV after B cell reconstitution, the presence of higher amounts of serum and airway IgG and partially impeded re-delivery in low-dose αCD20 further suggests that there may be a critical period after vector delivery during which there is

sufficient HAdV antigen remaining to stimulate an antibody response. Longer-term B cell depletion with high-dose αCD20 may have allowed sufficient time for antigen clearance before recovery, leading to a reduced antibody response. This hypothesis is supported by the finding of long-term airway persistence of HAdV antigen in studies using Nur77GFP reporter mice.[51] This suggests that the relative duration of vector antigen persistence and B cell depletion may be an important factor in the efficacy of preventing anti-vector responses. It will therefore be important to carefully assess vector pharmacokinetic data from human gene therapy trials as clinical immunosuppression protocols are designed. It is also worth noting that antigen load in the airway may decay at a different rate from circulating antigen, especially in the inflamed CF lung. Coupled with our observations that luminal rather than systemic antibody is more critical in limiting re-delivery, the duration of airway vector antigen persistence may be critical in determining the necessary duration of immunosuppression. We also observed no differences in antibody responses among low-dose αCD20 mice, which received a second dose of HAdV compared with those that did not undergo re-dosing. At our euthanasia time point of 3 days after secondary vector delivery, there may not have been sufficient time for development of a robust, detectable secondary antibody response. Another finding from this experiment was less impeded re-delivery (75% of vector-naive controls) in isotype-treated mice relative to prior experiments in which re-dosing was performed after 4 weeks (50% of vector naive controls). In this experiment, reduced inhibition of second-round gene transfer coupled with greater variability limited our ability to resolve statistically significant differences in transgene expression after secondary gene transfer. However, our results trended in a direction consistent with our prior results, with high-dose αCD20 yielding near complete restoration of second-round transgene expression. One possible explanation for less impeded re-delivery to isotype controls is that mucosal Ig responses, especially sIgA, are known to wane more quickly than systemic Ig responses upon antigen clearance.[52–55] Therefore, HAdV vector neutralization may have been less potent when re-dosing at 8 weeks rather than 4 weeks after primary HAdV delivery. While this may suggest that waiting for sufficient time may permit uninhibited re-delivery, it is worth noting that, in the chronically infected CF lung, IgA-producing plasmablasts often remain non-specifically activated, which may lead to a slower decline in mucosal humoral responses.[56]

Less certain impacts of αCD20 treatment on cell-mediated immunity were observed, for which there are several possible explanations. Firstly, T cell responses occur on a delayed timeline relative to pre-existing humoral immunity, and at euthanasia 3 days post delivery the influence of humoral immunity may dominate, limiting our ability to resolve differences in T cell responses. It is notable that our qPCR assay identified reduced vector genome copies in αCD20-treated mice that was not reflected in transgene enzymatic activity, which may be due to T cell-mediated elimination of transduced cells. Due to the kinetics of protein expression, transgene activity may reflect immediate-early transduction that is primarily impeded by humoral immune responses. These data suggest T cell responses in αCD20-treated mice may drive accelerated loss of transgene expression relative to second-vector-only mice in studies evaluating transgene persistence. Secondly, most of the expanded T cell clones we identified by sequencing were CD8+. While there is extensive literature on the relationship between CD4+ T cells and B cells, especially regarding B cell antigen presentation to CD4+ T cells through MHC class II, the interaction of B cells and CD8+ T cells is less studied.[57] While there are initial reports indicating a possible role for B cells in CD8+ T cell memory and recall responses,[58,59] we did not observe a large impact in our results, and some effects may be too subtle to observe without additional tools such as MHC class I tetramers. That said, we did observe some impacts of undetermined significance, with a reduction in the proportion of CD8+CD69+CD103+ T_{RM} and reduced numbers of all T cells detected in BALF. Together, these observations indicate that αCD20 may have had some impact on the formation of CD8+ T_{RM}, as the CD69+CD103+ population is thought to be enriched in "true" T_{RM}, and airway-infiltrating T cells found in BALF are primarily derived from T_{RM} progenitors.[60–63] However, further studies using more sensitive and specific immunological tools are needed to assess the significance of these findings.

Our scRNA-seq data also identified a pool of Th17 cells with a T_{RM}-like transcriptional profile in the lung 1 month after HAdV delivery. Many of these cells had not obviously undergone clonal expansion, suggesting that their presence may be related to the general inflammatory response resulting from HAdV delivery rather than a bona fide antigen-specific response. Interestingly, αCD20 treatment also appeared to impact the secretion of type 17 cytokines, suggesting a possible role for B cells in promoting generalized antiviral inflammation in the lung. Furthermore, given the importance of type 17 cells in mucosal immunity,[64] this also suggests that αCD20 treatment may have particular utility for inhaled gene therapy. However, most expanded T cell clones identified by scRNA-seq had an *Ifnγ*-expressing Th1 phenotype. As we found no differences with αCD20 in antigen-specific responses identified by IFN-γ ELISPOT assay, the observed changes in type 17 immunity may have limited functional impact. In future studies, we will investigate the impact of these changes and evaluate alternative interventions which may more effectively mitigate T cell responses to inhaled gene therapy vectors.

This study has several limitations. As mentioned previously, HAdV vectors are highly immunogenic and unlikely to be used as gene therapy vectors for gene replacement. Despite this, there is ongoing interest in using adenoviral vectors to deliver gene editing machinery due to larger payload capacity (∼30 kB) relative to AAV (∼5 kB).[65,66] The large carrying capacity of adenoviral vectors unlocks the possibility of all-in-one delivery for next-generation approaches such as prime editing or transposase-mediated gene insertion. However, rates of *in vivo* gene targeting are currently often too low for phenotypic correction, and the ability to repeatedly administer gene-modifying machinery could improve the feasibility of these approaches. It is worth noting that T cell responses against transduced cells in a gene-modifying context are likely to remain a barrier to long-term gene expression.

With the success of this proof-of-concept study, our future work will extend to evaluating clinically relevant AAV vectors. An additional concern for treatment efficacy is that the inflammatory environment of the CF lung may present unique challenges for gene delivery, as inflammation has been proposed to underlie treatment failure in AAV gene therapy trials for muscular dystrophy.[67–69] In CF, chronic inflammation also results in the formation of airway-associated tertiary lymphoid structures termed inducible bronchus-associated lymphoid tissue (iBALT),[15] which may present an environment primed for robust anti-vector immune responses. Clinically, αCD20 treatment initiated prior to lung transplantation in two pwCF was insufficient to reduce iBALT,[22] suggesting that these cells may not re-circulate. This study is supported by experiments in mice noting that previously established B_{RM} are not depleted by αCD20 treatment.[22] The possibility of non-re-circulating B cells in iBALT raises the concern that the advantage of αCD20 treatment in lung-directed vector delivery relative to systemic vector delivery may be less significant in pwCF. Future experiments will attempt to address the unique challenges presented by gene transfer to the CF lung, especially in the context of clinically relevant AAV vectors.

MATERIALS AND METHODS

Mice

Six- to 8-week-old WT C57BL/6J mice were obtained from The Jackson Laboratory (Bar Harbor, ME). Genetically modified $FcRn^{-/-}$, $AID^{-/-}$, and $\mu S^{-/-}$ mice were similarly obtained from the Jackson Laboratory (Bar Harbor, ME). $AID^{-/-}$ $\mu S^{-/-}$ mice were generated by crossing $AID^{-/-}$ and $\mu S^{-/-}$ strains to obtain mice homozygous for knockout of both alleles.[38] $IgA^{-/-}$ mice were a kind gift from Dr. Elisabeth Norton. Mice were maintained at the Tulane University Department of Comparative Medicine Facility. Animals were housed in a pathogen-free environment and given food and water ad libitum. All experiments were approved by the Tulane University Animal Care and Use Committee.

Antibody treatment and adenoviral vector inoculation

Mice were dosed with the indicated quantity of anti-mouse CD20-depleting antibody (clone 5D2, murine IgG2a, Genentech) or isotype control (clone C1.18.4, murine IgG2a, BioXCell) by intraperitoneal injection 2 days prior to vector delivery. HAdV-GFP (cat. no. 1060) and HAdV-LacZ (cat. no. 1080) adenoviral vectors were either obtained from Vector Biolabs. HAdV-empty and HAdV-Luc vectors were produced in 293 cells and purified by CsCl gradient ultracentrifugation as described previously.[70] Mice were inoculated with either 10^9 PFU (HAdV-GFP and HAdV-Luc) or 5×10^{10} vector genomes (Ad-empty) by oral-pharyngeal aspiration (tongue-pull method).[47]

Single-cell isolation from lungs and BAL

At the time of euthanasia, mice were anesthetized with isoflurane, then injected with 2 μg of anti-mouse CD45.2 PE (BioLegend, cat. no. 109807). Two minutes later, mice were euthanized by CO_2 asphyxiation. BAL was collected by instillation and recovery of 1 mL of 0.2 mM EDTA in PBS. PBS/EDTA was instilled and recovered 3 times, with a typical yield of 750 μL. BAL was spun down, the supernatant was frozen for ELISA analysis and the cell pellet was washed for flow cytometric staining. Subsequently, one or both lungs were removed, minced with dissection scissors, and digested in IMDM (Gibco) with 2 mg/mL collagenase (Sigma) and 20 U/mL DNAse-1 (Sigma) at 37°C for 60–90 min with gentle rotation. Digested tissue solution was filtered through a 70-μm cell strainer (Fisherbrand), and red blood cells were removed by ACK lysis (Gibco).

Flow cytometry

Single-cell suspensions of lung cells and BAL were washed with ice-cold PBS, then re-suspended in PBS containing a 1:8,000 dilution of Ghost Dye Red 780 (Tonbo, cat. no. 13-0865-T100) for 20 min. All washes were performed by centrifugation at $300 \times g$ for 5 min prior to fixation and $500 \times g$ for 5 min post fixation. Cells were washed once with FACS Buffer (PBS + 1% BSA, Gemini Bio), then re-suspended in FACS buffer containing a 1:100 dilution of Fc Block (BD, cat. no. 553142) and a 1:20 dilution of True-Stain Monocyte Blocker (BioLegend, cat. no. 426103). After 10 min, an equal volume of FACS buffer containing a 1:50 dilution of anti-mouse CD69 BV421 (BD, cat. no. 562920) and CD103 BV711 (BD, cat. no. 748255) with 10 μL/sample of Brilliant Stain Buffer Plus (BD, cat. no. 566385) was added, and cells were stained for 30 min. Cells were washed once with FACS buffer and re-suspended in 2% paraformaldehyde (Thermo Fisher, cat. no. 28906) for 20 min. After fixation, cells were washed once with FACS buffer and re-suspended in pooled antibody-staining solution containing 10 μL/sample of Brilliant Stain Buffer Plus (BD, cat. no. 566385), a 1:20 dilution of True-Stain Monocyte Blocker (BioLegend, cat. no. 426103), and the following anti-mouse antibodies at the following dilutions: 1:640 CD3 PE-Cy5 (BD, cat. no. 553065), 1:10,240 CD4 PE-Cy7 (BD, cat. no. 552775), 1:2,560 CD8 APC (BD, cat. no. 553035), 1:1,280 CD19 BV750 (BD, cat. no. 747332), 1:640 IgM BV510 (BD, cat. no. 743324), 1:640 IgD BV605 (BD, cat. no. 563003), 1:2,560 CD38 Alexa Fluor 700 (BioLegend, cat. no. 102741). Cells were stained overnight,[71] then washed and resuspended in FACS buffer before acquisition. For enumeration of peripheral blood lymphocytes, 10 μL of blood obtained by retro-orbital bleeding was stained with a 1:100 dilution of the following anti-mouse antibodies for 20 min: CD45.2 Alexa Fluor 700 (BioLegend, cat. no. 109821) or PE (BioLegend, cat. no. 109807), CD3 PE-Cy5 (BD, cat. no. 553065), CD4 PE-Cy7 (BD, cat. no. 552775), CD8 APC (BD, cat. no. 553035), CD19 BB515 (BD, cat. no. 564531). One hundred and ten microliters of 1X eBioscience Fix/Lyse (Thermo Fisher, cat. no. 00-5333-54) was added and samples were allowed to undergo fixation and RBC lysis for 20 min. Subsequently, 125 μL of FACS buffer was added, and 150 μL of sample was acquired. Cytometric analyses were performed with a Cytek Aurora (Cytek Biosciences) and analyzed using FlowJo v.10 software (Ashland, OR).

ELISPOT and LegendPlex analysis

IFN-γ ELISPOT was carried out on single cells isolated from mice 4 weeks after HAdV delivery according to the manufacturer's instructions (Mabtech, 3321-2A) as a measure of Th1 responses. Cells were stimulated overnight with the dominant peptide H2-Kb CTL epitope

for HAdV,[34] luciferase,[35] or PMA/Ionomycin (Thermo Fisher, cat. no. 00-4970-93). ELISPOT supernatants were spun down to remove cells and saved at −80°C for LEGENDplex analysis. LEGENDplex assay was carried out according to manufacturer's instructions (BioLegend, cat. no. 741044), using the centrifugation protocol. Data acquisition was performed on a Cytek Aurora and analyzed using the LEGENDplex Data Analysis Software Suite (BioLegend). For B cell ELISPOT, ethanol-activated plates (Millipore Sigma, cat. no. MAIPS4510) were coated with HAdV at a concentration of 2×10^{11} vp/mL in PBS. Isolated lung cells were pre-stimulated for 72 h with R848 at 1 μg/mL and rmIL-2 at 10 ng/mL before being transferred to the antigen-coated plate. Cells were incubated overnight, then plates were processed according to the manufacturer's instructions (Mabtech, IgA: 3865-2A; IgG: 3865-2A). ELISPOT plates were developed with 1-Step NBT/BCIP Substrate Solution (Thermo Fisher, cat. no. 34042), imaged with an S6 Macro ELISPOT (Cellular Technology Limited) plate reader and counted with ImmunoSpot v.7 software (Cellular Technology Limited). ELISPOT signal was analyzed after subtraction of background spots in unstimulated wells. Due to higher background in the B cell ELISPOT assay, spots in wells containing cells from naive control mice were used to apply background subtraction. The dotted line indicates the mean + 3 SD of the level in naive control mice. Flow cytometric enumeration of T cells was used for normalization of LegendPlex data.

ELISA

High-binding assay plates were coated overnight at 4°C with 2×10^{10} vg/mL of HAdV in carbonate-coating buffer (100 mM [pH 9.6]). After coating, plates were washed 5 times with 0.05% PBS-T, then blocked for 2 h at room temperature with 1% BSA (Gemini Bio) in 0.1% PBS-T. BAL and serum samples were diluted in 0.5% BSA and 0.05% PBS-T, then applied to the plate for 1 h at room temperature. Plates were then washed 5 times with 0.05% PBS-T, and HRP-conjugated anti-mouse IgG (Southern Biotech, cat. no. 1030-05) or IgA (Southern Biotech, cat. no. 1040-05) detection antibodies diluted 1:4,000 were applied to the plate for 30 min. After 5 washes, plates were developed with TMB substrate solution (Thermo Fisher, cat. no. N301) for 15 min before stopping development with an equal volume of 0.2 M H_2SO_4. OD450 was measured using a BioTek Synergy HT microplate reader (Agilent Biosciences). Assay background was subtracted using naive mouse serum as negative control samples. Dotted lines are given as mean + 3 SD of the naive control.

Single-cell V(D)J and 5′ gene expression sequencing

Intravascular CD45-PE-labeled single-cell lung suspension was subjected to depletion using anti-PE microbeads (Miltenyi, cat. no. 130-408-801), then positive selection using a mouse CD3ε microbead kit (Miltenyi, cat. no. 130-094-973) according to the manufacturer's instructions. Cell numbers and viability were validated by Nexcelom Cellometer Auto 2000 (Nexcelom Bioscience) and AO/PI viability dye (Nexcelom Bioscience, cat. no. CS2-0106) prior to preparation of single-cell RNA-seq library. To perform the 10X single-cell V(D)J seq assay, 5,000 live cells per sample were used to create GEMs by combining barcoded Single Cell 5′ Gel Beads (10X Genomics, cat. no. 1000265). After GEM-RT, RT cleanup, full-length cDNA amplification and QC, T cell receptor-enriched libraries, and 5′ gene expression libraries were generated with Illumina P5 and P7 adapters. The libraries were quality controlled using Agilent High Sensitive DNA kit (Agilent, cat. no. 5067-4626) with Agilent 2100 Bioanalyzer (Agilent, cat. no. G2939BA) and quantified by Qubit 2.0 fluorometer (Thermo Fisher, cat. no. Q32886). Finally, the pooled libraries were sequenced with paired-end dual index configuration by Illumina NextSeq 2000 (Illumina) at a final concentration of 750 pM. Cell Ranger v.7.1 (10X Genomics) was used to process raw sequencing data integrated with a publicly available naive spleen dataset (10X Genomics, https://www.10xgenomics.com/resources/datasets/integrated-gex-and-vdj-analysis-of-connect-generated-library-from-mouse-splenocytes-2-standard-6-0-1). Loupe Cell Browser 6 (10X Genomics) was used to cluster cells and evaluate differentially expressed genes between specified cell clusters. In brief, T cells were evaluated by re-clustering on cells with associated TCR clonotype sequences positive for CD3e and negative for Mzb1, CD209e, Jchain, and Mzb1 expression. CD8+ T cells were identified by selecting cells positive for CD8a expression, and CD4+ T cells were defined by CD8a negativity, as CD4 mRNA expression is known to be a less-reliable marker for cell identification. After identification of CD4+ and CD8+ T cells, clusters were analyzed for expression of candidate genes as described. GEO accession number is GSE261943.

LacZ, luciferase, and BCA assays

Gal-Screen β-Galactosidase Reporter Gene Assay System (Invitrogen, cat. no. T1027) and the One-Glo Luciferase Assay System (Promega, cat. no. E6110) were used to assay gene transfer efficiency, according to the manufacturer's instructions. During euthanasia, mice were injected with PBS into the right ventricle to clear the lung of circulating peripheral blood. The left lung was collected into Lysing Matrix D tubes (MP Biomedicals, cat. no. 116913100) containing 1 mL of either 100 mM K-phosphate (pH 7.8), 0.2% Triton X-100, 1 mM dithiothreitol, and 1× proteinase inhibitor cocktail[72] for LacZ activity assay or Glo Lysis Buffer (Promega, cat. no. E2661). Tissue was homogenized using a FastPrep-24 5G bead beating grinder and lysis system (MP Biomedicals, cat. no. 116005500) and stored at −80°C until analysis. For the LacZ activity assay, 100 μL of lung homogenate diluted 1:100 in potassium phosphate buffer was mixed with 100 μL prepared Gal-Screen substrate and incubated for 1 h at room temperature before acquisition. For the One-Glo Luciferase Assay, 100 μL of undiluted lung homogenate was mixed with 100 μL of reconstituted One-Glo Luciferase Assay Buffer and incubated for 5 min at room temperature before acquisition. Both activity assays were performed in 96-well U-bottom white plates (Corning, cat. no. 3355) and luminescent activity was measured using a BioTek Synergy HT microplate reader with auto-gain and a 1 s integration time. Sample protein concentration was quantified with Pierce BCA Protein Assay (Thermo Fisher, cat. no. 23225) according to the manufacturer's instructions. Samples were diluted 1:5 in PBS and 25 μL of diluted sample was mixed with 200 μL of working reagent and incubated for 30 min at 37°C. Absorbance at 562 nm was measured using a BioTek Synergy HT microplate reader.

qPCR

DNA from mouse lung homogenate in 100 mM K-phosphate (pH 7.8), 0.2% Triton X-100, 1 mM dithiothreitol, and 1× proteinase inhibitor cocktail was isolated by spin-column purification (Zymo, cat. no. D7001). Ten nanograms DNA was used in a 20 μL PCR reaction (TaqMan universal PCR Master Mix, cat. no. 4304437) detecting *LacZ* (TaqMan, assay ID no. Mr03987581_mr) and mouse Tfrc as a reference assay (TaqMan, cat. no. 4458366). Data were collected using a Bio-Rad CFX Opus 96 Real-Time PCR System and analyzed using Bio-Rad CFX Maestro qPCR Analysis Software.

Histology

In experiments where histology was performed, at euthanasia after BAL, the right main bronchus was tied off using silk suture (Fine Science Tools, cat. no. 18020-00). Then, the left lobe was inflated with zinc-buffered formalin (Z-Fix, Anatech, cat. no. 170), tied off, removed, and fixed for 36–48 h in zinc-buffered formalin, then embedded in paraffin. Lung sections (4 μm) were stained with hematoxylin and eosin. Serial unstained sections were incubated at 60°C to melt the paraffin. The remaining paraffin was removed by immersion in xylene, and sections were rehydrated through graded alcohol. Antigen retrieval was performed with citrate buffer (10 mM sodium citrate, 0.05% Tween 20 [pH 6.0]) in a pressure cooker for 20 min. Slides were processed using the VECTASTAIN Elite ABC-HRP Kit (cat. no. PK-6101, Vector Biolabs) according to the manufacturer's instructions, modified to incubate overnight with rabbit anti-β-galactosidase primary antibody (cat. no. PM049, MBL International) at a 1:4,000 dilution. Slides were developed using a DAB metal-enhanced substrate kit (Thermo Fisher, cat. no. 34065). After development, slides were washed in PBS and mounted with VectaMount Permanent Mounting Media (Vector Biolabs, cat. no. H-5000) followed by imaging on an Olympus BX53 microscope.

Statistics

All statistics were calculated using GraphPad Prism (version 9.5.1). *p* values of less than 0.05 were considered significant.

DATA AND CODE AVAILABILITY

Sequencing data are available on the Gene Expression Omnibus (GSE261943). All additional data are available upon request.

SUPPLEMENTAL INFORMATION

Supplemental information can be found online at https://doi.org/10.1016/j.omtm.2024.101286.

ACKNOWLEDGMENTS

We would like to thank Kejing Song, and Mst Shamima Khatun in the CTRII NGS core for helping with the single-cell NGS data. We would also like to acknowledge the technical assistance from Ms. Connie Porretta in the Tulane Flow Cytometry Core and assay support from Dr. Haoran Yang and Dr. Alexis Katz. We thank Genentech for providing 5D2 for these studies. This work was supported by NIH R35HL 139930, NIH TL1 TR003106, the Louisiana Board of Regents Endowed Chairs for Eminent Scholars program, and CF Foundation Awards (KOLLS23G0). The content is solely the responsibility of the authors and does not necessarily represent the official views of the National Institutes of Health.

AUTHOR CONTRIBUTIONS

R.D.E.C. designed and performed experiments, analyzed data, and wrote the manuscript. F.R., F.T.M., and T.P.R. performed experiments and edited the manuscript. J.K.K. conceived the study, designed experiments, and wrote the manuscript.

DECLARATION OF INTERESTS

The authors declare no competing interests.

REFERENCES

1. Collawn, J.F., and Matalon, S. (2014). CFTR and lung homeostasis. Am. J. Physiol. Lung Cell Mol. Physiol. *307*, L917–L923. https://doi.org/10.1152/ajplung.00326.2014.
2. O'Sullivan, B.P., and Freedman, S.D. (2009). Cystic fibrosis. Lancet *373*, 1891–1904. https://doi.org/10.1016/s0140-6736(09)60327-5.
3. Veit, G., Avramescu, R.G., Chiang, A.N., Houck, S.A., Cai, Z., Peters, K.W., Hong, J.S., Pollard, H.B., Guggino, W.B., Balch, W.E., et al. (2016). From CFTR biology toward combinatorial pharmacotherapy: expanded classification of cystic fibrosis mutations. Mol. Biol. Cell *27*, 424–433. https://doi.org/10.1091/mbc.e14-04-0935.
4. Wainwright, C.E., Elborn, J.S., Ramsey, B.W., Marigowda, G., Huang, X., Cipolli, M., Colombo, C., Davies, J.C., De Boeck, K., Flume, P.A., et al. (2015). Lumacaftor–Ivacaftor in Patients with Cystic Fibrosis Homozygous for Phe508del CFTR. N. Engl. J. Med. *373*, 220–231. https://doi.org/10.1056/NEJMoa1409547.
5. Middleton, P.G., Mall, M.A., Dřevínek, P., Lands, L.C., McKone, E.F., Polineni, D., Ramsey, B.W., Taylor-Cousar, J.L., Tullis, E., Vermeulen, F., et al. (2019). Elexacaftor–Tezacaftor–Ivacaftor for Cystic Fibrosis with a Single Phe508del Allele. N. Engl. J. Med. *381*, 1809–1819. https://doi.org/10.1056/NEJMoa1908639.
6. Harrison, M.J., Murphy, D.M., and Plant, B.J. (2013). Ivacaftor in a G551D Homozygote with Cystic Fibrosis. N. Engl. J. Med. *369*, 1280–1282. https://doi.org/10.1056/NEJMc1213681.
7. Elborn, J.S., Ramsey, B.W., Boyle, M.P., Konstan, M.W., Huang, X., Marigowda, G., Waltz, D., and Wainwright, C.E.; VX-809 TRAFFIC and TRANSPORT study groups (2016). Efficacy and safety of lumacaftor/ivacaftor combination therapy in patients with cystic fibrosis homozygous for Phe508del CFTR by pulmonary function subgroup: a pooled analysis. Lancet Respir. Med. *4*, 617–626. https://doi.org/10.1016/S2213-2600(16)30121-7.
8. Choi, S.H., and Engelhardt, J.F. (2021). Gene Therapy for Cystic Fibrosis: Lessons Learned and Paths Forward. Mol. Ther. *29*, 428–430. https://doi.org/10.1016/j.ymthe.2021.01.010.
9. Yang, Y., Li, Q., Ertl, H.C., and Wilson, J.M. (1995). Cellular and humoral immune responses to viral antigens create barriers to lung-directed gene therapy with recombinant adenoviruses. J. Virol. *69*, 2004–2015. https://doi.org/10.1128/jvi.69.4.2004-2015.1995.
10. Griesenbach, U., and Alton, E.W.F.W. (2013). Moving forward: cystic fibrosis gene therapy. Hum. Mol. Genet. *22*, R52–R58. https://doi.org/10.1093/hmg/ddt372.
11. Künzli, M., and Masopust, D. (2023). CD4+ T cell memory. Nat. Immunol. *24*, 903–914. https://doi.org/10.1038/s41590-023-01510-4.
12. Allie, S.R., Bradley, J.E., Mudunuru, U., Schultz, M.D., Graf, B.A., Lund, F.E., and Randall, T.D. (2019). The establishment of resident memory B cells in the lung requires local antigen encounter. Nat. Immunol. *20*, 97–108. https://doi.org/10.1038/s41590-018-0260-6.
13. Barker, K.A., Etesami, N.S., Shenoy, A.T., Arafa, E.I., Lyon de Ana, C., Smith, N.M., Martin, I.M., Goltry, W.N., Barron, A.M., Browning, J.L., et al. (2021). Lung-resident memory B cells protect against bacterial pneumonia. J. Clin. Invest. *131*, e141810. https://doi.org/10.1172/JCI141810.
14. Rangel-Moreno, J., Carragher, D.M., de la Luz Garcia-Hernandez, M., Hwang, J.Y., Kusser, K., Hartson, L., Kolls, J.K., Khader, S.A., and Randall, T.D. (2011). The

development of inducible bronchus-associated lymphoid tissue depends on IL-17. Nat. Immunol. *12*, 639–646. https://doi.org/10.1038/ni.2053.

15. Rangel-Moreno, J., Hartson, L., Navarro, C., Gaxiola, M., Selman, M., and Randall, T.D. (2006). Inducible bronchus-associated lymphoid tissue (iBALT) in patients with pulmonary complications of rheumatoid arthritis. J. Clin. Invest. *116*, 3183–3194. https://doi.org/10.1172/JCI28756.

16. Leborgne, C., Barbon, E., Alexander, J.M., Hanby, H., Delignat, S., Cohen, D.M., Collaud, F., Muraleetharan, S., Lupo, D., Silverberg, J., et al. (2020). IgG-cleaving endopeptidase enables *in vivo* gene therapy in the presence of anti-AAV neutralizing antibodies. Nat. Med. *26*, 1096–1101. https://doi.org/10.1038/s41591-020-0911-7.

17. Elmore, Z.C., Oh, D.K., Simon, K.E., Fanous, M.M., and Asokan, A. (2020). Rescuing AAV gene transfer from neutralizing antibodies with an IgG-degrading enzyme. JCI Insight *5*, e139881. https://doi.org/10.1172/jci.insight.139881.

18. Bertin, B., Veron, P., Leborgne, C., Deschamps, J.-Y., Moullec, S., Fromes, Y., Collaud, F., Boutin, S., Latournerie, V., van Wittenberghe, L., et al. (2020). Capsid-specific removal of circulating antibodies to adeno-associated virus vectors. Sci. Rep. *10*, 864. https://doi.org/10.1038/s41598-020-57893-z.

19. Orlowski, A., Katz, M.G., Gubara, S.M., Fargnoli, A.S., Fish, K.M., and Weber, T. (2020). Successful Transduction with AAV Vectors after Selective Depletion of Anti-AAV Antibodies by Immunoadsorption. Mol. Ther. Methods Clin. Dev. *16*, 192–203. https://doi.org/10.1016/j.omtm.2020.01.004.

20. Mingozzi, F., Maus, M.V., Hui, D.J., Sabatino, D.E., Murphy, S.L., Rasko, J.E.J., Ragni, M.V., Manno, C.S., Sommer, J., Jiang, H., et al. (2007). CD8+ T-cell responses to adeno-associated virus capsid in humans. Nat. Med. *13*, 419–422. https://doi.org/10.1038/nm1549.

21. Chirmule, N., Truneh, A., Haecker, S.E., Tazelaar, J., Gao, G.-P., Raper, S.E., Hughes, J.V., and Wilson, J.M. (1999). Repeated administration of adenoviral vectors in lungs of human CD4 transgenic mice treated with a nondepleting CD4 antibody. J. Immunol. *163*, 448–455. https://doi.org/10.4049/jimmunol.163.1.448.

22. Regard, L., Martin, C., Zemoura, L., Geolier, V., Sage, E., and Burgel, P.-R. (2018). Peribronchial tertiary lymphoid structures persist after rituximab therapy in patients with cystic fibrosis. J. Clin. Pathol. *71*, 752–753. https://doi.org/10.1136/jclinpath-2018-205160.

23. Reynaud-Gaubert, M., Stoppa, A.M., Gaubert, J., Thomas, P., and Fuentes, P. (2000). Anti-CD20 monoclonal antibody therapy in Epstein-Barr virus–associated B cell lymphoma following lung transplantation. J. Heart Lung Transplant. *19*, 492–495. https://doi.org/10.1016/S1053-2498(00)00087-5.

24. Hirche, T.O., Knoop, C., Hebestreit, H., Shimmin, D., Solé, A., Elborn, J.S., Ellemunter, H., Aurora, P., Hogardt, M., and Wagner, T.O.F.; ECORN-CF Study Group (2014). Practical Guidelines: Lung Transplantation in Patients with Cystic Fibrosis. Pulm. Med. *2014*, 621342. https://doi.org/10.1155/2014/621342.

25. Elsegeiny, W., Eddens, T., Chen, K., and Kolls, J.K. (2015). Anti-CD20 Antibody Therapy and Susceptibility to Pneumocystis Pneumonia. Infect. Immun. *83*, 2043–2052. https://doi.org/10.1128/iai.03099-14.

26. Pattinson, D., Jester, P., Guan, L., Yamayoshi, S., Chiba, S., Presler, R., Rao, H., Iwatsuki-Horimoto, K., Ikeda, N., Hagihara, M., et al. (2022). A Novel Method to Reduce ELISA Serial Dilution Assay Workload Applied to SARS-CoV-2 and Seasonal HCoVs. Viruses *14*, 562.

27. Anderson, K.G., Mayer-Barber, K., Sung, H., Beura, L., James, B.R., Taylor, J.J., Qunaj, L., Griffith, T.S., Vezys, V., Barber, D.L., and Masopust, D. (2014). Intravascular staining for discrimination of vascular and tissue leukocytes. Nat. Protoc. *9*, 209–222. https://doi.org/10.1038/nprot.2014.005.

28. Skon, C.N., Lee, J.-Y., Anderson, K.G., Masopust, D., Hogquist, K.A., and Jameson, S.C. (2013). Transcriptional downregulation of S1pr1 is required for the establishment of resident memory CD8+ T cells. Nat. Immunol. *14*, 1285–1293. https://doi.org/10.1038/ni.2745.

29. Steinert, E.M., Schenkel, J.M., Fraser, K.A., Beura, L.K., Manlove, L.S., Igyártó, B.Z., Southern, P.J., and Masopust, D. (2015). Quantifying Memory CD8 T Cells Reveals Regionalization of Immunosurveillance. Cell *161*, 737–749. https://doi.org/10.1016/j.cell.2015.03.031.

30. Kumar, B.V., Ma, W., Miron, M., Granot, T., Guyer, R.S., Carpenter, D.J., Senda, T., Sun, X., Ho, S.-H., Lerner, H., et al. (2017). Human Tissue-Resident Memory T Cells Are Defined by Core Transcriptional and Functional Signatures in Lymphoid and Mucosal Sites. Cell Rep. *20*, 2921–2934. https://doi.org/10.1016/j.celrep.2017.08.078.

31. Beura, L.K., Fares-Frederickson, N.J., Steinert, E.M., Scott, M.C., Thompson, E.A., Fraser, K.A., Schenkel, J.M., Vezys, V., and Masopust, D. (2019). CD4+ resident memory T cells dominate immunosurveillance and orchestrate local recall responses. J. Exp. Med. *216*, 1214–1229. https://doi.org/10.1084/jem.20181365.

32. Szabo, P.A., Miron, M., and Farber, D.L. (2019). Location, location, location: Tissue resident memory T cells in mice and humans. Sci. Immunol. *4*, eaas9673. https://doi.org/10.1126/sciimmunol.aas9673.

33. Hirahara, K., Kokubo, K., Aoki, A., Kiuchi, M., and Nakayama, T. (2021). The Role of CD4+ Resident Memory T Cells in Local Immunity in the Mucosal Tissue – Protection Versus Pathology. Front. Immunol. *12*, 616309. https://doi.org/10.3389/fimmu.2021.616309.

34. McKelvey, T., Tang, A., Bett, A.J., Casimiro, D.R., and Chastain, M. (2004). T-cell response to adenovirus hexon and DNA-binding protein in mice. Gene Ther. *11*, 791–796. https://doi.org/10.1038/sj.gt.3302232.

35. Limberis, M.P., Bell, C.L., and Wilson, J.M. (2009). Identification of the murine firefly luciferase-specific CD8 T-cell epitopes. Gene Ther. *16*, 441–447. https://doi.org/10.1038/gt.2008.177.

36. Choi, S.J., Yi, J.S., Lim, J.-A., Tedder, T.F., Koeberl, D.D., Jeck, W., Desai, A.K., Rosenberg, A., Sun, B., and Kishnani, P.S. (2023). Successful AAV8 readministration: Suppression of capsid-specific neutralizing antibodies by a combination treatment of bortezomib and CD20 mAb in a mouse model of Pompe disease. J. Gene Med. *25*, e3509. https://doi.org/10.1002/jgm.3509.

37. He, W., Ladinsky, M.S., Huey-Tubman, K.E., Jensen, G.J., McIntosh, J.R., and Björkman, P.J. (2008). FcRn-mediated antibody transport across epithelial cells revealed by electron tomography. Nature *455*, 542–546. https://doi.org/10.1038/nature07255.

38. Kumazaki, K., Tirosh, B., Maehr, R., Boes, M., Honjo, T., and Ploegh, H.L. (2007). AID-/-mus-/- mice are agammaglobulinemic and fail to maintain B220-CD138+ plasma cells. J. Immunol. *178*, 2192–2203. https://doi.org/10.4049/jimmunol.178.4.2192.

39. Delorey, T.M., Ziegler, C.G.K., Heimberg, G., Normand, R., Yang, Y., Segerstolpe, Å., Abbondanza, D., Fleming, S.J., Subramanian, A., Montoro, D.T., et al. (2021). COVID-19 tissue atlases reveal SARS-CoV-2 pathology and cellular targets. Nature *595*, 107–113. https://doi.org/10.1038/s41586-021-03570-8.

40. Lu, H.-F., Zhou, Y.-C., Yang, L.-T., Zhou, Q., Wang, X.-J., Qiu, S.-Q., Cheng, B.-H., and Zeng, X.-H. (2024). Involvement and repair of epithelial barrier dysfunction in allergic diseases. Front. Immunol. *15*, 1348272. https://doi.org/10.3389/fimmu.2024.1348272.

41. Huang, Q., Le, Y., Li, S., and Bian, Y. (2024). Signaling pathways and potential therapeutic targets in acute respiratory distress syndrome (ARDS). Respir. Res. *25*, 30. https://doi.org/10.1186/s12931-024-02678-5.

42. Shirley, J.L., de Jong, Y.P., Terhorst, C., and Herzog, R.W. (2020). Immune Responses to Viral Gene Therapy Vectors. Mol. Ther. *28*, 709–722. https://doi.org/10.1016/j.ymthe.2020.01.001.

43. Ozelo, M.C., Mahlangu, J., Pasi, K.J., Giermasz, A., Leavitt, A.D., Laffan, M., Symington, E., Quon, D.V., Wang, J.-D., Peerlinck, K., et al. (2022). Valoctocogene Roxaparvovec Gene Therapy for Hemophilia A. N. Engl. J. Med. *386*, 1013–1025. https://doi.org/10.1056/NEJMoa2113708.

44. Rosato, P.C., Lotfi-Emran, S., Joag, V., Wijeyesinghe, S., Quarnstrom, C.F., Degefu, H.N., Nedellec, R., Schenkel, J.M., Beura, L.K., Hangartner, L., et al. (2023). Tissue resident memory T cells trigger rapid exudation and local antibody accumulation. Mucosal Immunol. *16*, 17–26. https://doi.org/10.1016/j.mucimm.2022.11.004.

45. Farber, D.L. (2020). Form and function for T cells in health and disease. Nat. Rev. Immunol. *20*, 83–84. https://doi.org/10.1038/s41577-019-0267-8.

46. Kushwah, R., Cao, H., and Hu, J. (2008). Characterization of pulmonary T cell response to helper-dependent adenoviral vectors following intranasal delivery. J. Immunol. *180*, 4098–4108. https://doi.org/10.4049/jimmunol.180.6.4098.

47. Dai, G., Noell, K., Weckbecker, G., and Kolls, J.K. (2021). Effect of Subcutaneous Anti-CD20 Antibody-Mediated B Cell Depletion on Susceptibility to Pneumocystis Infection in Mice. mSphere *6*, e01144-20. https://doi.org/10.1128/msphere.01144-20.

48. Meliani, A., Boisgerault, F., Hardet, R., Marmier, S., Collaud, F., Ronzitti, G., Leborgne, C., Costa Verdera, H., Simon Sola, M., Charles, S., et al. (2018). Antigen-selective modulation of AAV immunogenicity with tolerogenic rapamycin nanoparticles enables successful vector re-administration. Nat. Commun. *9*, 4098. https://doi.org/10.1038/s41467-018-06621-3.

49. Montalvao, F., Garcia, Z., Celli, S., Breart, B., Deguine, J., Van Rooijen, N., and Bousso, P. (2013). The mechanism of anti-CD20–mediated B cell depletion revealed by intravital imaging. J. Clin. Invest. *123*, 5098–5103. https://doi.org/10.1172/JCI70972.

50. Häusler, D., Häusser-Kinzel, S., Feldmann, L., Torke, S., Lepennetier, G., Bernard, C.C.A., Zamvil, S.S., Brück, W., Lehmann-Horn, K., and Weber, M.S. (2018). Functional characterization of reappearing B cells after anti-CD20 treatment of CNS autoimmune disease. Proc. Natl. Acad. Sci. USA *115*, 9773–9778. https://doi.org/10.1073/pnas.1810470115.

51. Uddbäck, I., Cartwright, E.K., Schøller, A.S., Wein, A.N., Hayward, S.L., Lobby, J., Takamura, S., Thomsen, A.R., Kohlmeier, J.E., and Christensen, J.P. (2021). Long-term maintenance of lung resident memory T cells is mediated by persistent antigen. Mucosal Immunol. *14*, 92–99. https://doi.org/10.1038/s41385-020-0309-3.

52. Diallo, B.K., Ní Chasaide, C., Wong, T.Y., Schmitt, P., Lee, K.S., Weaver, K., Miller, O., Cooper, M., Jazayeri, S.D., Damron, F.H., and Mills, K.H.G. (2023). Intranasal COVID-19 vaccine induces respiratory memory T cells and protects K18-hACE mice against SARS-CoV-2 infection. npj Vaccines *8*, 68. https://doi.org/10.1038/s41541-023-00665-3.

53. Renson, P., Mahé, S., Andraud, M., Le Dimna, M., Paboeuf, F., Rose, N., and Bourry, O. (2024). Effect of vaccination route (intradermal vs. intramuscular) against porcine reproductive and respiratory syndrome using a modified live vaccine on systemic and mucosal immune response and virus transmission in pigs. BMC Vet. Res. *20*, 5. https://doi.org/10.1186/s12917-023-03853-4.

54. Sheikh-Mohamed, S., Isho, B., Chao, G.Y.C., Zuo, M., Cohen, C., Lustig, Y., Nahass, G.R., Salomon-Shulman, R.E., Blacker, G., Fazel-Zarandi, M., et al. (2022). Systemic and mucosal IgA responses are variably induced in response to SARS-CoV-2 mRNA vaccination and are associated with protection against subsequent infection. Mucosal Immunol. *15*, 799–808. https://doi.org/10.1038/s41385-022-00511-0.

55. Denis, J., Garnier, A., Cheutin, L., Ferrier, A., Timera, H., Jarjaval, F., Hejl, C., Billon-Denis, E.; Percy ImmunoCovid group, and Ricard, D., et al. (2023). Long-term systemic and mucosal SARS-CoV-2 IgA response and its association with persistent smell and taste disorders. Front. Immunol. *14*, 1140714. https://doi.org/10.3389/fimmu.2023.1140714.

56. Collin, A.M., Lecocq, M., Noel, S., Detry, B., Carlier, F.M., Aboubakar Nana, F., Bouzin, C., Leal, T., Vermeersch, M., De Rose, V., et al. (2020). Lung immunoglobulin A immunity dysregulation in cystic fibrosis. EBioMedicine *60*, 102974. https://doi.org/10.1016/j.ebiom.2020.102974.

57. Adler, L.N., Jiang, W., Bhamidipati, K., Millican, M., Macaubas, C., Hung, S.-C., and Mellins, E.D. (2017). The Other Function: Class II-Restricted Antigen Presentation by B Cells. Front. Immunol. *8*, 319. https://doi.org/10.3389/fimmu.2017.00319.

58. Klarquist, J., Cross, E.W., Thompson, S.B., Willett, B., Aldridge, D.L., Caffrey-Carr, A.K., Xu, Z., Hunter, C.A., Getahun, A., and Kedl, R.M. (2021). B cells promote CD8 T cell primary and memory responses to subunit vaccines. Cell Rep. *36*, 109591. https://doi.org/10.1016/j.celrep.2021.109591.

59. Graalmann, T., Borst, K., Manchanda, H., Vaas, L., Bruhn, M., Graalmann, L., Koster, M., Verboom, M., Hallensleben, M., Guzmán, C.A., et al. (2021). B cell depletion impairs vaccination-induced CD8+ T cell responses in a type I interferon-dependent manner. Ann. Rheum. Dis. *80*, 1537–1544. https://doi.org/10.1136/annrheumdis-2021-220435.

60. Zheng, M.Z.M., and Wakim, L.M. (2022). Tissue resident memory T cells in the respiratory tract. Mucosal Immunol. *15*, 379–388. https://doi.org/10.1038/s41385-021-00461-z.

61. Uddbäck, I., Michalets, S.E., Saha, A., Mattingly, C., Kost, K.N., Williams, M.E., Lawrence, L.A., Hicks, S.L., Lowen, A.C., Ahmed, H., et al. (2024). Prevention of respiratory virus transmission by resident memory CD8+ T cells. Nature *626*, 392–400. https://doi.org/10.1038/s41586-023-06937-1.

62. Takamura, S., Kato, S., Motozono, C., Shimaoka, T., Ueha, S., Matsuo, K., Miyauchi, K., Masumoto, T., Katsushima, A., Nakayama, T., et al. (2019). Interstitial-resident memory CD8+ T cells sustain frontline epithelial memory in the lung. J. Exp. Med. *216*, 2736–2747. https://doi.org/10.1084/jem.20190557.

63. McMaster, S.R., Wilson, J.J., Wang, H., and Kohlmeier, J.E. (2015). Airway-Resident Memory CD8 T Cells Provide Antigen-Specific Protection against Respiratory Virus Challenge through Rapid IFN-γ Production. J. Immunol. *195*, 203–209. https://doi.org/10.4049/jimmunol.1402975.

64. Kolls, J.K., and Khader, S.A. (2010). The role of Th17 cytokines in primary mucosal immunity. Cytokine Growth Factor Rev. *21*, 443–448. https://doi.org/10.1016/j.cytogfr.2010.11.002.

65. Cooney, A.L., Singh, B.K., and Sinn, P.L. (2015). Hybrid Nonviral/Viral Vector Systems for Improved piggyBac DNA Transposon In Vivo Delivery. Mol. Ther. *23*, 667–674. https://doi.org/10.1038/mt.2014.254.

66. Bandara, R.A., Chen, Z.R., and Hu, J. (2021). Potential of helper-dependent Adenoviral vectors in CRISPR-cas9-mediated lung gene therapy. Cell Biosci. *11*, 145. https://doi.org/10.1186/s13578-021-00662-w.

67. Ferrand, M., Galy, A., and Boisgerault, F. (2014). A dystrophic muscle broadens the contribution and activation of immune cells reacting to rAAV gene transfer. Gene Ther. *21*, 828–839. https://doi.org/10.1038/gt.2014.61.

68. Mendell, J.R., Campbell, K., Rodino-Klapac, L., Sahenk, Z., Shilling, C., Lewis, S., Bowles, D., Gray, S., Li, C., Galloway, G., et al. (2010). Dystrophin Immunity in Duchenne's Muscular Dystrophy. N. Engl. J. Med. *363*, 1429–1437. https://doi.org/10.1056/NEJMoa1000228.

69. Boisgerault, F., and Mingozzi, F. (2015). The Skeletal Muscle Environment and Its Role in Immunity and Tolerance to AAV Vector-Mediated Gene Transfer. Curr. Gene Ther. *15*, 381–394. https://doi.org/10.2174/1566523215666150630121750.

70. Kolls, J., Peppel, K., Silva, M., and Beutler, B. (1994). Prolonged and effective blockade of tumor necrosis factor activity through adenovirus-mediated gene transfer. Proc. Natl. Acad. Sci. USA *91*, 215–219. https://doi.org/10.1073/pnas.91.1.215.

71. Whyte, C.E., Tumes, D.J., Liston, A., and Burton, O.T. (2022). Do more with Less: Improving High Parameter Cytometry Through Overnight Staining. Curr. Protoc. *2*, e589. https://doi.org/10.1002/cpz1.589.

72. Koehler, D.R., Martin, B., Corey, M., Palmer, D., Ng, P., Tanswell, A.K., and Hu, J. (2006). Readministration of helper-dependent adenovirus to mouse lung. Gene Ther. *13*, 773–780. https://doi.org/10.1038/sj.gt.3302712.